

## Supporting Information

### All-Metal $\sigma$ -Antiaromaticity in Dimeric Cluster Anion $\{[\text{CuGe}_9\text{Mes}]_2\}^{4-}$

Zi-Chuan Wang, Nikolay V. Tkachenko, Lei Qiao, Eduard Matito, Alvaro Muñoz-Castro, Alexander I. Boldyrev,\* and Zhong-Ming Sun\*

Antiaromaticity is used to describe the instability of delocalized system featured with  $4n$  electrons. Few corresponding compounds have been found in condensed phase, especially for the  $\sigma$ -antiaromatic inorganic compound which has never been synthesized in the solid state. In this work, we report a dimeric cluster anion  $\{[\text{CuGe}_9\text{Mes}]_2\}^{4-}$ , which was isolated as the  $[\text{K}([2.2.2]\text{crypt})]^+$  salt and characterized by single-crystal X-ray diffraction and ESI mass spectrum. Based on theoretical analysis, we conclude that the  $\{[\text{CuGe}_9\text{Mes}]_2\}^{4-}$  cluster has a local  $\sigma$ -antiaromatic  $\text{Cu}_2\text{Ge}_2$  unit stabilized by two multiple  $\sigma$ -aromatic  $\text{Ge}_9$  clusters with the  $\pi$ -aromaticity of mesityl group. The title cluster represents the first locally  $\sigma$ -antiaromatic compound in the solid state, as well as the first heteroatomic antiaromatic compound.

## Table of Contents

Synthesis Details .....	2
Crystallographic Supplementation .....	2
Energy Dispersive X-ray (EDX) Spectroscopic Analysis .....	5
Mechanism study .....	5
Optimized geometries of investigated molecules and additional computational results .....	8
Computational methods .....	13
References .....	14

## Synthesis Details

All manipulations were performed under N<sub>2</sub> atmospheres using glovebox or standard Schlenk-lines techniques. N,N-dimethylformamide (Aldrich, 99.8%) and toluene (Aldrich, 99.8%) were distilled by sodium in a nitrogen atmosphere and stored in a glove box prior to use. 4,7,13,16,21,24-Hexaoxa-1,10-diazabicyclo[8.8.8]hexacosane ([2,2,2]-crypt, Sigma-Aldrich 98%) were dried under vacuum for several hours and transfer to glovebox for use. "K<sub>4</sub>Ge<sub>9</sub>" was a nominal stoichiometric powder synthesized by heating a mixture of the elements at 800 °C for three days in a sealed niobium tube. CuMes (Mes=2,4,6-trimethylphenyl) was synthesized under anhydrous and anaerobic conditions according to the reported literature procedure<sup>1</sup>.

### X-ray Diffraction.

Suitable single crystals were selected for X-ray diffraction analyses. Crystallographic data were collected on Rigaku XtalAB Pro MM007 DW diffractometer with graphite monochromated Cu K $\alpha$  radiation ( $\lambda$  = 1.54184 Å). Structures were solved using direct methods and then refined using SHELXL-2014 and Olex2<sup>2-4</sup> to convergence, in which all the non-hydrogen atoms were refined anisotropically during the final cycles. All hydrogen atoms of the organic molecule were placed by geometrical considerations and were added to the structure factor calculation. Positional disorder was found in the cluster site in compound 1, and this was modeled accordingly (see Figure 3, 4). A summary of the crystallographic data for these complexes is listed in Table S2, and selected bond distances are given in Table S3. CCDC 1974758 contains the supplementary crystallographic data for this paper. These data can be obtained free of charge from The Cambridge Crystallographic Data Centre ([www.ccdc.cam.ac.uk/data\\_request/cif](http://www.ccdc.cam.ac.uk/data_request/cif)).

### Electrospray Ionization Mass Spectrometry (ESI-MS) Investigations.

ESI-MS of the single crystal of compound 1 were performed on Agilent Technologies ESI-TOF-MS (6230). The crystals of 1 were dissolved in dry MeCN inside a glovebox under N<sub>2</sub> atmosphere and rapidly transferred to the spectrometer in an air-tight syringe by direct infusion with a Harvard syringe pump at 208  $\mu$ L/min, capillary temperature 300 °C.

### Synthesis of [K(2,2,2-crypt)]<sub>4</sub>[CuGe<sub>9</sub>Mes]<sub>2</sub>(dmf)<sub>3</sub> (1):

CuMes (52 mg, 0.28 mmol) was added in 3 mL DMF solution of K<sub>4</sub>Ge<sub>9</sub> (113 mg, 0.14 mmol). The reaction was stirred for 3 hours at 50 °C. The solvent was removed by vacuum, and the residue was washed with THF before resolving in 1.5 mL dmf. Then, another CuMes (26 mg, 0.14 mmol) was added. After 3 h reaction at 65 °C, the dark-reddish brown solution was filtered and layered by 1.5 mL toluene carefully. Red block-shaped crystals can be obtained after 3 days and examined by single-crystal X-ray diffraction.

## Crystallographic Supplementation

**Table S1** X-ray measurements and structure solution of compounds.

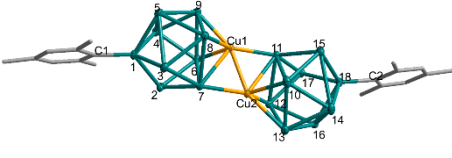
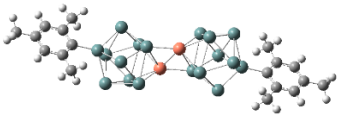
Compound	1
Empirical formula	C <sub>18</sub> H <sub>22</sub> Cu <sub>2</sub> Ge <sub>18</sub> ·4(C <sub>18</sub> H <sub>36</sub> KN <sub>2</sub> O <sub>6</sub> )·3(C <sub>3</sub> H <sub>7</sub> NO)
Formula weight	3553.68
Temperature/K	153
Crystal system	triclinic
Space group	<i>P</i> $\bar{1}$
a/Å	15.32218(12)
b/Å	19.01622(16)
c/Å	25.9169(2)
$\alpha$ /°	100.0676(7)
$\beta$ /°	101.7388(7)
$\gamma$ /°	105.5044(7)
Volume/Å <sup>3</sup>	6910.99(10)

Z	2
$\rho_{\text{calc}}/\text{g}/\text{cm}^3$	1.707
$\mu/\text{mm}^{-1}$	6.225
F(000)	3568.0
Crystal size/ $\text{mm}^3$	$0.18 \times 0.16 \times 0.15$
Radiation	$\text{CuK}\alpha$ ( $\lambda = 1.54184$ )
2 $\theta$ range for data collection/ $^\circ$	5.38 to 147.32
Index ranges	$-18 \leq h \leq 19, -23 \leq k \leq 12, -28 \leq l \leq 32$
Reflections collected	78372
Independent reflections	26999 [ $R_{\text{int}} = 0.0326, R_{\text{sigma}} = 0.0334$ ]
Data/restraints/parameters	26999/1/1463
Goodness-of-fit on $F^2$	1.023
Final R indexes [ $ I  > 2\sigma(I)$ ]	$R_1 = 0.0403, wR_2 = 0.1031$
Final R indexes [all data]	$R_1 = 0.0468, wR_2 = 0.1062$
Largest diff. peak/hole / $\text{e } \text{\AA}^{-3}$	1.71/-0.81

$$^b R_1 = \sum ||F_o| - |F_c|| / \sum |F_o|; wR_2 = \{ \sum w[(F_o)^2 - (F_c)^2]^2 / \sum w(F_o)^2 \}^{1/2}$$

$$^b \text{GooF} = \{ \sum w[(F_o)^2 - (F_c)^2]^2 / (n-p) \}^{1/2}$$

**Table S2.** Selected interatomic distances (in  $\text{\AA}$ ) of the experimental and optimized structures of the cluster **1** at the PBE0/Def2-TZVP level of theory.

	Experimental	Optimized
		
Cu1—Cu2	2.5214 (7)	2.58866
Ge1—C1	1.998(3)	2.02172
Ge1—Ge2	2.5000 (5)	2.53799
Ge1—Ge3	2.5105 (6)	2.53799
Ge1—Ge4	2.5618 (5)	2.57617
Ge1—Ge5	2.5425 (5)	2.57617
Ge2—Ge6	2.5026 (5)	2.52142
Ge2—Ge7	2.5441 (5)	2.56392
Ge3—Ge5	2.9354 (6)	2.94593
Ge3—Ge7	2.5386 (6)	2.56392
Ge3—Ge8	2.5027 (6)	2.52142
Ge4—Ge9	2.5796 (6)	2.59282
Ge5—Ge4	2.8171 (6)	2.84405
Ge5—Ge8	2.6412 (6)	2.63513
Ge5—Ge9	2.5705 (6)	2.59282
Ge6—Cu1	2.4361 (6)	2.49182
Ge6—Ge7	2.7999 (6)	2.80534
Ge7—Cu1	2.6072 (6)	2.61512
Ge7—Cu2	2.4007 (6)	2.47681
Ge7—Ge8	2.7450 (6)	2.80534
Ge8—Cu1	2.4478 (6)	2.49182
Ge8—Ge9	2.6854 (6)	2.70342
Ge9—Cu1	2.6260 (6)	2.78540
Ge9—Ge6	2.7325(6)	2.70342
Ge10—Cu2	2.4583 (7)	2.49182
Ge10—Ge11	2.7731 (6)	2.80534
Ge10—Ge14	2.5984 (6)	2.63513
Ge10—Ge15	2.5222 (6)	2.52142
Ge11—Cu1	2.4301 (6)	2.47681
Ge11—Cu2	2.5998 (6)	2.61512
Ge11—Ge12	2.7543 (6)	2.80534

Ge11—Ge15	2.5648 (6)	2.56392
Ge11—Ge17	2.5447 (6)	2.56392
Ge12—Cu2	2.4425 (7)	2.49182
Ge12—Ge16	2.5984 (6)	2.63513
Ge12—Ge17	2.5161 (6)	2.52142
Ge14—Ge15	2.8915 (6)	2.94593
Ge14—Ge16	2.8864 (6)	2.84405
Ge14—Ge18	2.5369 (6)	2.57617
Ge15—Ge18	2.5189 (6)	2.53799
Ge16—Ge18	2.5325 (6)	2.57617
Ge17—Ge18	2.4945 (6)	2.53799
Ge18—C2	1.993 (3)	2.02172



**Figure S1.** Crystals of **1**.

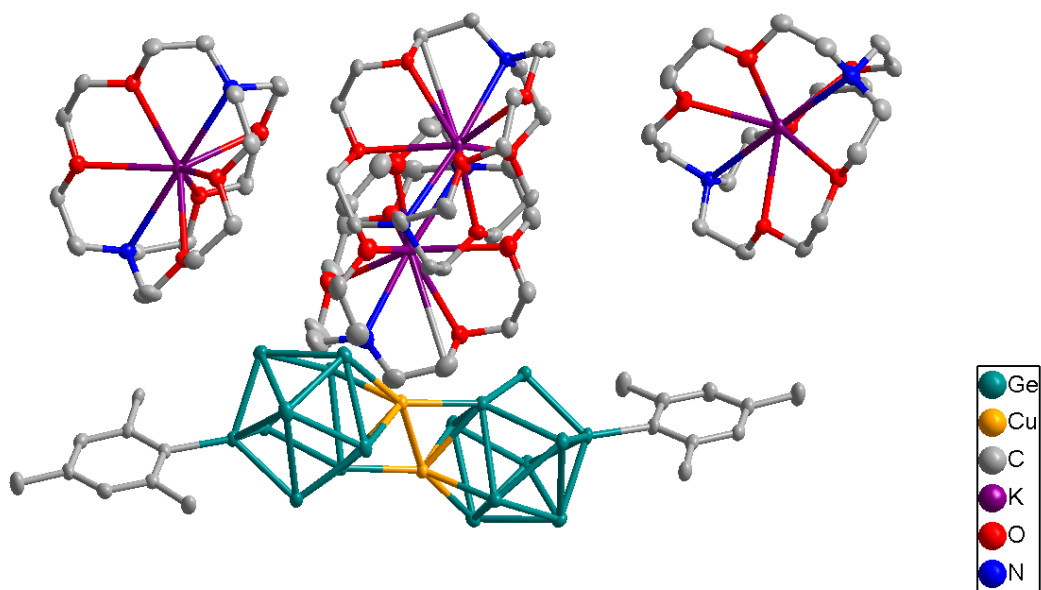


**Figure S2.** Asymmetric unit of **1** with the cluster fragment. Thermal ellipsoids are drawn at 50% probability. The minor components are omitted for clarity.

## Energy Dispersive X-ray (EDX) Spectroscopic Analysis

EDX analysis of **1** (Figure S3) was performed using a scanning electron microscope (FE-SEM, JEOL JSM-7800F, Japan). Data acquisition was performed with an acceleration voltage of 15 kV and an accumulation time of 60 s. The molar ratio of K/Cu/Ge is 2.0:1.14:9.0, which is a little deviation but in a reasonable range of error with the experimental crystallographic data.

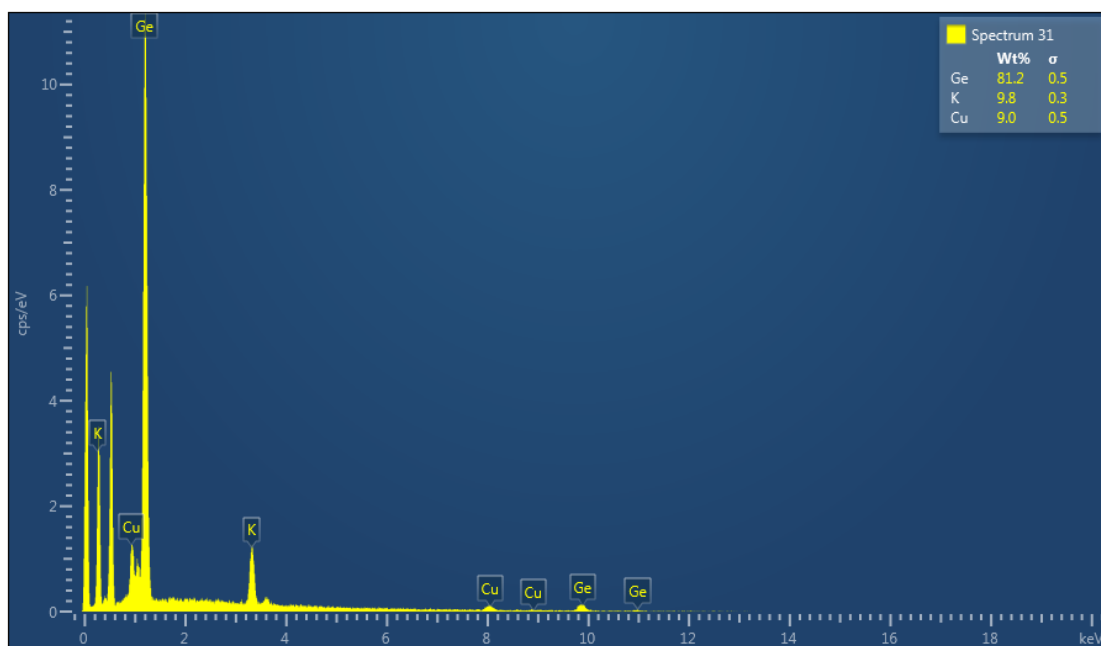


Figure S3. EDX analysis of **1** (K, Cu, Ge).

## Mechanism study

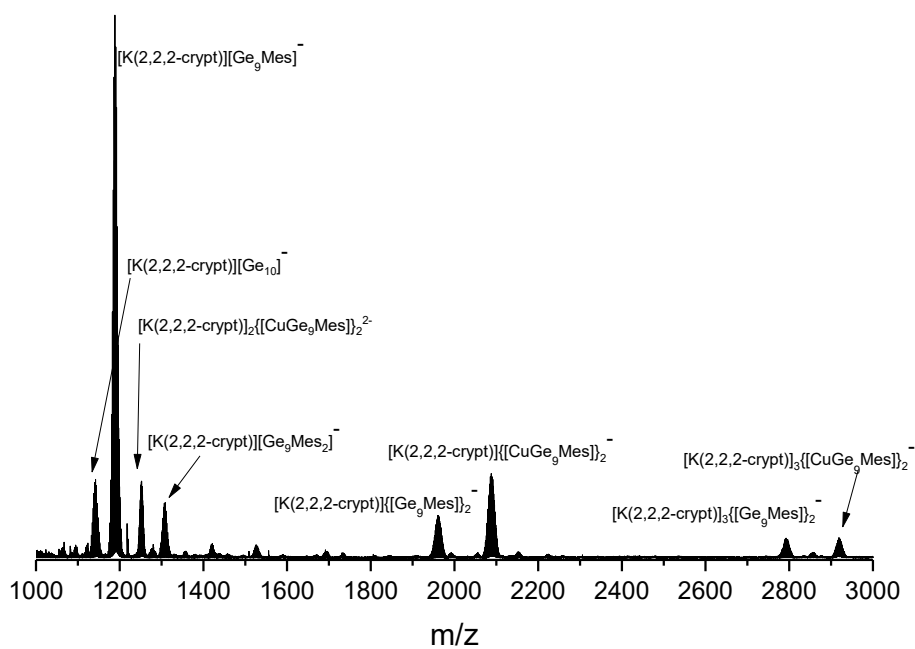
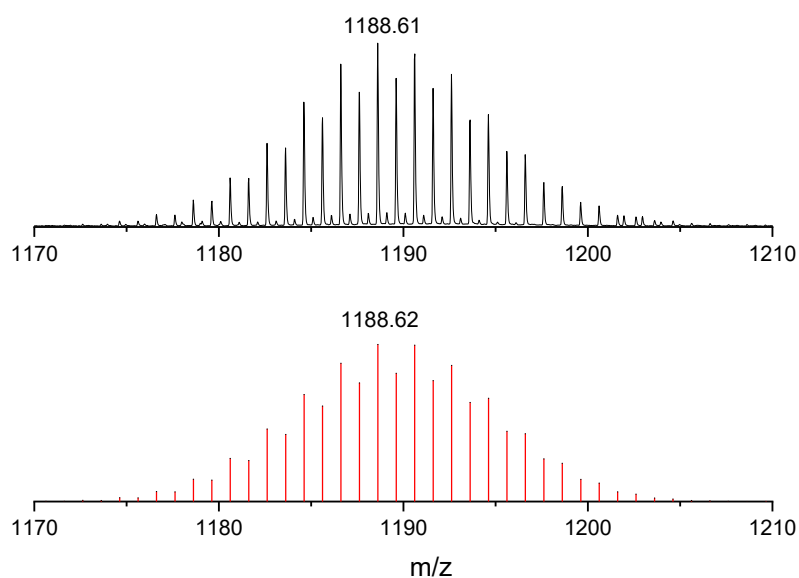
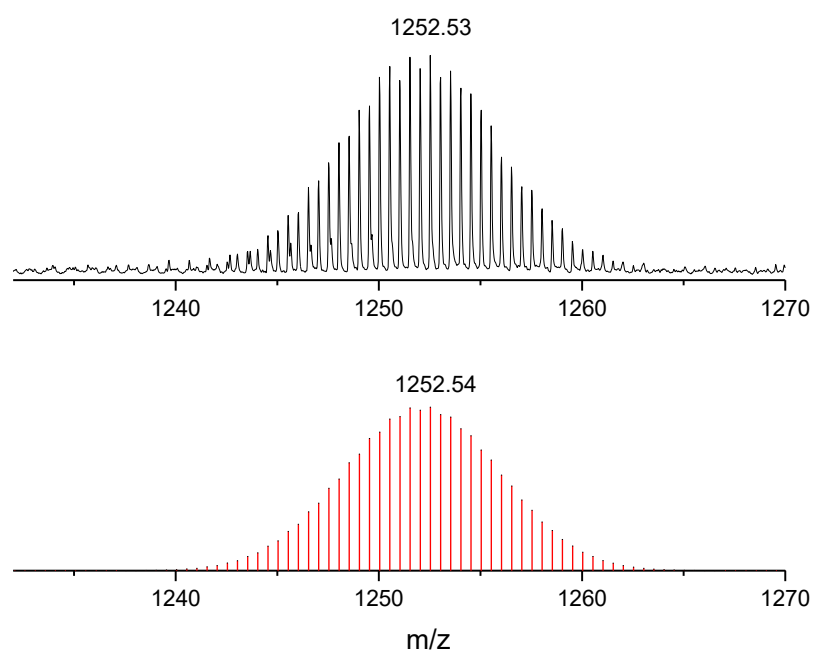


Figure S4. Negative ion mode ESI-MS ( $m/z$ : 1000-3000) of a dissolved of **1** in MeCN.



**Figure S5.** Measured (top) and simulated (bottom) spectrum of the fragment  $[K(2,2,2\text{-crypt})][Ge_9Mes]^-$



**Figure S6.** Measured (top) and simulated (bottom) spectrum of the fragment  $[K(2,2,2\text{-crypt})]_2\{[CuGe_9Mes]\}_2^{2-}$

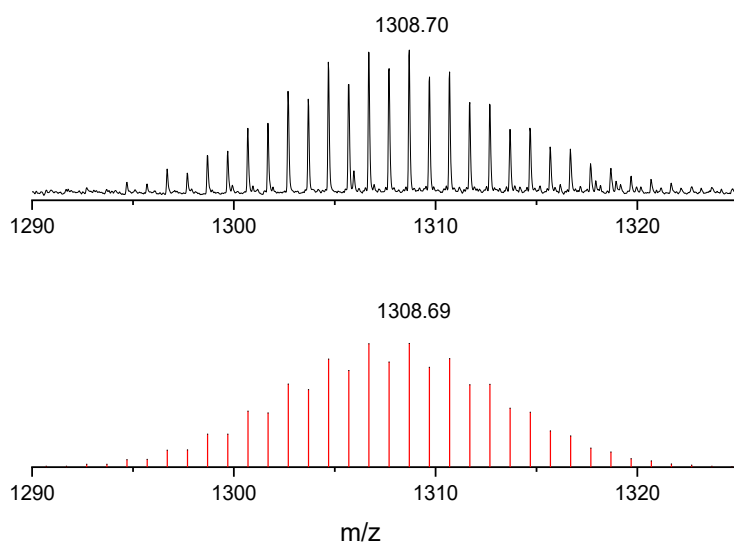


**Figure S7.** Measured (top) and simulated (bottom) spectrum of the fragment  $[K(2,2,2\text{-crypt})][Ge_9Mes_2]^-$

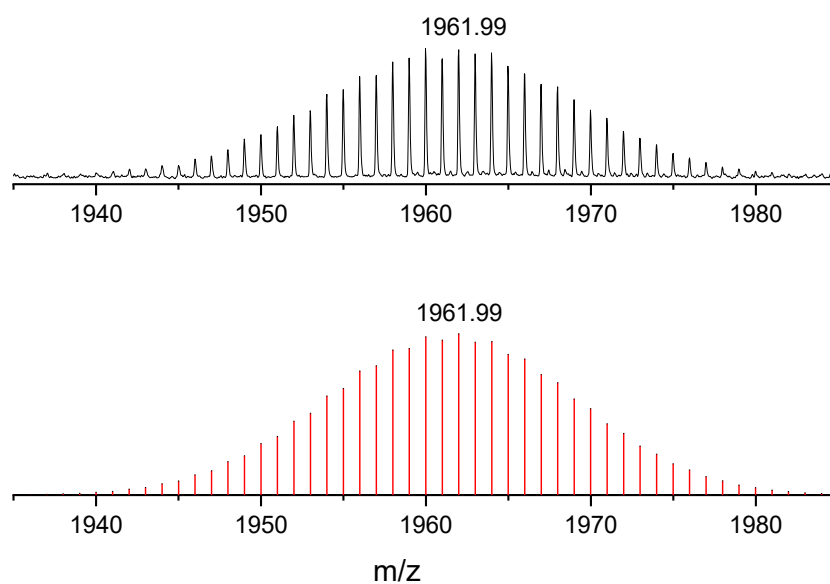


**Figure S8.** Measured (top) and simulated (bottom) spectrum of the fragment  $[K(2,2,2\text{-crypt})][Ge_{18}Mes_2]^-$

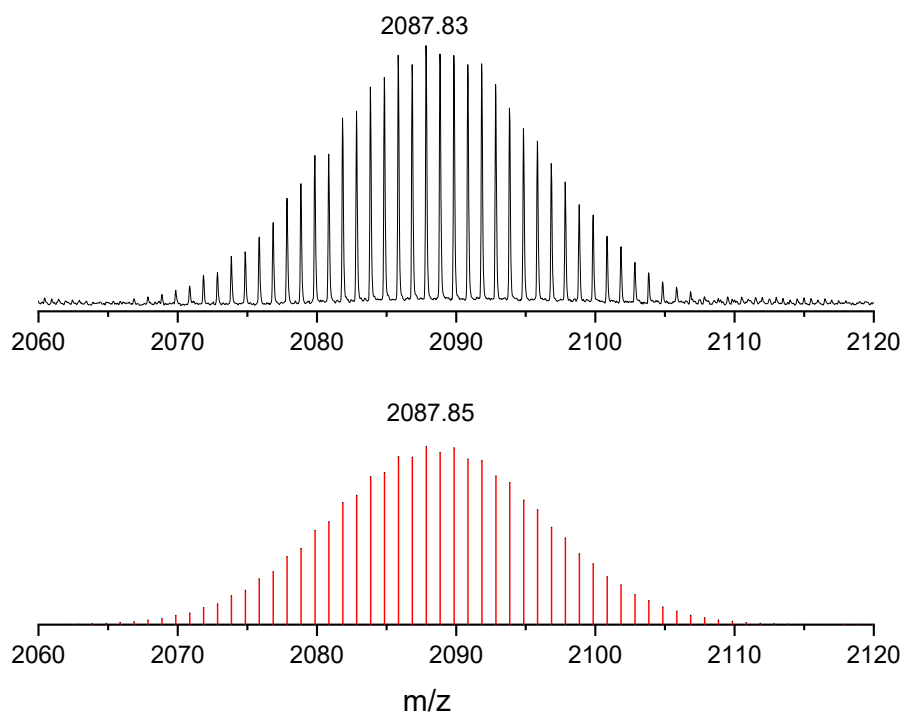


**Figure S9.** Measured (top) and simulated (bottom) spectrum of the fragment  $[K(2,2,2\text{-crypt})][Cu_2Ge_{18}Mes_2]^+$

## Optimized geometries of investigated molecules and additional computational results

**Table S3.** Coordinates (Å) of optimized geometries, total energies and ZPE corrections (a.u.) of investigated molecules.

$C_s [CuGe_9Mes]^{2-}$ (singlet)	PBE0/Def2-TZVP (0 imaginary Frequencies, $E_{elec} = -20680.6294103$ , ZPE correction= 0.180740)		
	32	-1.523579000	-0.010299000
	32	-2.057937000	-2.004692000
	32	0.002649000	-2.008230000
	32	0.002649000	-2.008230000
	32	-1.523579000	-0.010299000
	29	0.005334000	-3.305007000
	32	-0.003729000	1.312204000
	32	1.520871000	-0.004299000
	32	2.063259000	-1.996352000
	32	1.520871000	-0.004299000
	6	-0.007049000	4.035338000
	6	-0.008780000	5.428955000
	6	-0.007049000	4.035338000
	6	-0.012098000	3.345101000
	6	-0.008780000	5.428955000
	6	-0.006179000	6.147620000
	6	0.029615000	7.648381000
	1	-0.883815000	2.690499000
	1	0.858533000	2.689907000
	1	-0.014262000	4.072120000
	1	-0.014732000	5.965754000
	1	0.858533000	2.689907000
	1	-0.883815000	2.690499000
	1	-0.014262000	4.072120000
	1	-0.014732000	5.965754000
	1	-0.465394000	8.058124000
	1	1.058872000	8.027047000
	1	-0.465394000	8.058124000
	6	-0.012098000	3.345101000
	6	-0.004483000	3.313413000



C <sub>2h</sub> {[CuGe <sub>9</sub> Mes] <sub>2</sub> } <sup>4-</sup> (singlet)	PBE0/Def2-TZVP (0 imaginary Frequencies, E <sub>elec</sub> = -41361.0931945, ZPE correction= 0.360296)		
	32	-0.995447000	2.193514000
	32	0.988169000	3.747696000
	32	1.072217000	1.913575000
	32	-1.072217000	-1.913575000
	32	0.995447000	-2.193514000
	32	0.237909000	5.383509000
	32	-2.852997000	2.778026000
	32	0.988169000	3.747696000
	32	-0.988169000	-3.747696000
	32	-0.995447000	2.193514000
	32	-0.988169000	-3.747696000
	32	-0.237909000	-5.383509000
	32	-1.786797000	4.665825000
	32	-1.786797000	4.665825000
	32	1.786797000	-4.665825000
	32	1.786797000	-4.665825000
	32	2.852997000	-2.778026000
	32	0.995447000	-2.193514000
	29	-1.166220000	0.561450000
	29	1.166220000	-0.561450000
	6	0.806103000	8.078393000
	6	-0.637624000	-7.365326000
	6	0.806103000	8.078393000
	6	-0.806103000	-8.078393000
	6	1.306182000	10.134486000
	6	-1.132611000	-9.433842000
	1	-1.250117000	-9.956771000
	6	0.637624000	7.365326000
	6	-0.806103000	-8.078393000
	6	0.629639000	7.410968000
	1	-0.371381000	6.974528000
	1	1.315679000	6.564549000
	1	0.791953000	8.119111000
	6	1.132611000	9.433842000
	1	1.250117000	9.956771000
	6	-1.306182000	-10.134486000
	6	0.629639000	7.410968000
	1	1.315679000	6.564549000
	1	-0.371381000	6.974528000
	1	0.791953000	8.119111000
	6	1.132611000	9.433842000
	1	1.250117000	9.956771000
	6	-1.697993000	-11.584129000
	1	-2.788434000	-11.716253000
	1	-1.312524000	-12.100489000
	1	-1.312524000	-12.100489000
	6	-1.132611000	-9.433842000
	1	-1.250117000	-9.956771000
	6	1.697993000	11.584129000
	1	1.312524000	12.100489000
	1	2.788434000	11.716253000
	1	1.312524000	12.100489000
	6	-0.629639000	-7.410968000
	1	0.371381000	-6.974528000
	1	-1.315679000	-6.564549000
	1	-0.791953000	-8.119111000
	6	-0.629639000	-7.410968000
	1	-1.315679000	-6.564549000
	1	0.371381000	-6.974528000
	1	-0.791953000	-8.119111000

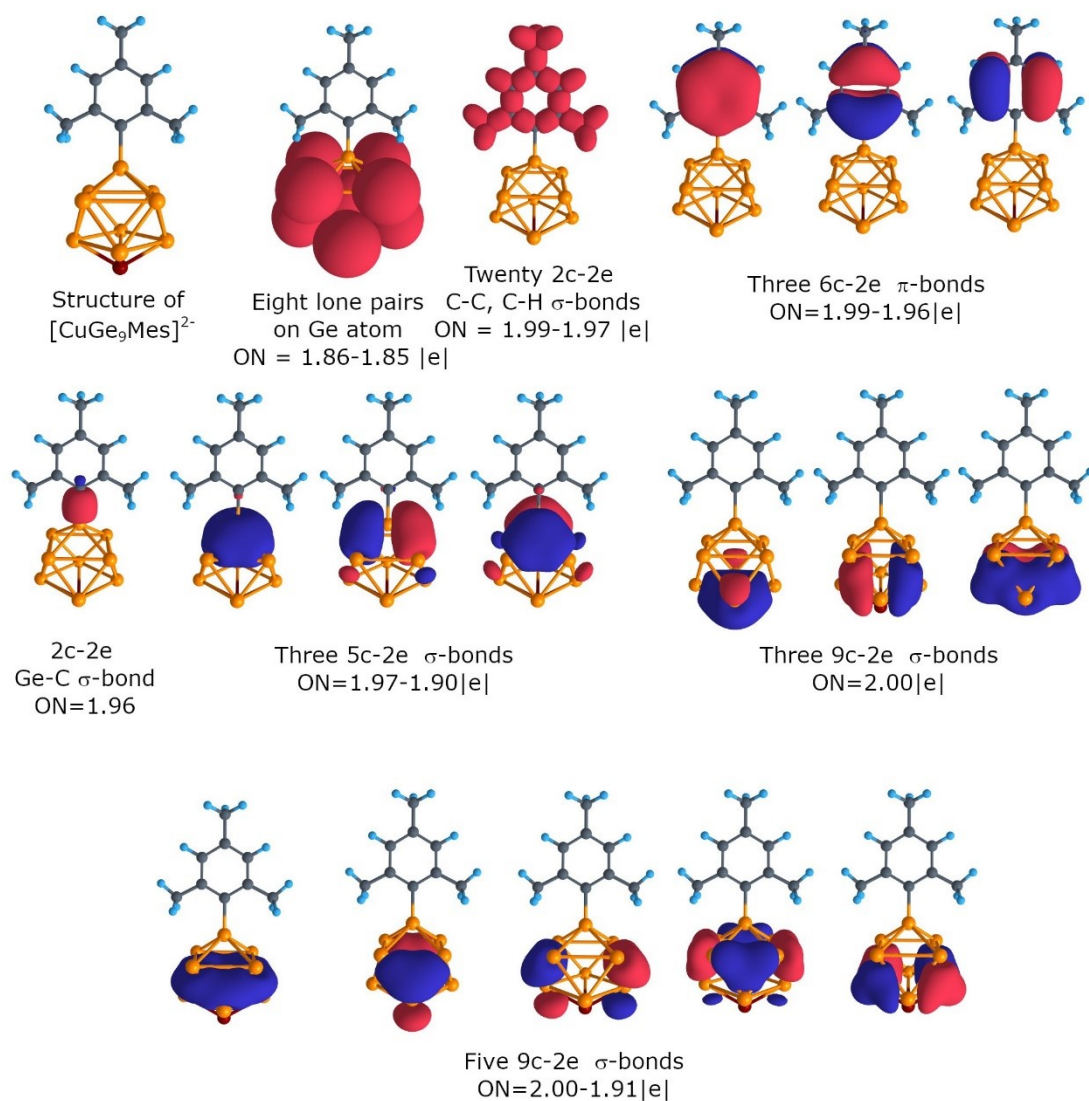


**Figure S10.** Overall chemical bonding picture obtained for the  $[\text{CuGe}_9\text{Mes}]^{2-}$  cluster

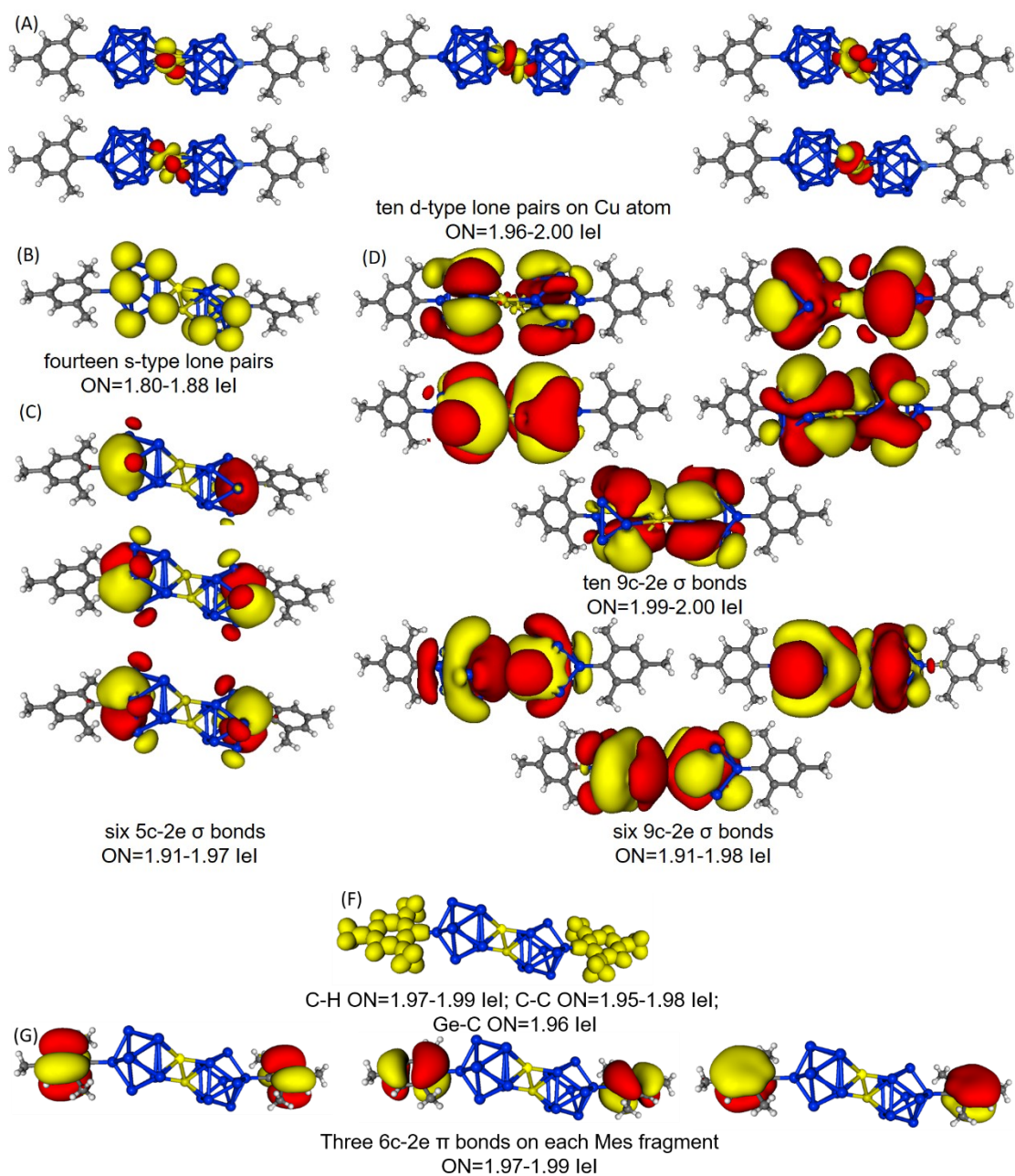


**Figure S11.** Overall chemical bonding picture obtained for the  $\{[\text{CuGe}_9\text{Mes}]_2\}^{4-}$  cluster. A) 5 d-type LPs on each Cu atoms ( $d_{z^2}$ ,  $d_{xy}$ ,  $d_{yz}$ ,  $d_{xz}$  and  $d_{x^2-y^2}$ ) B) 14 s-type LPs on 14 Ge atoms; C) 6 5c-2e  $\sigma$  bonds ( $\text{Ge}_5$ ); D) 10 9c-2e  $\sigma$  bonds ( $\text{CuGe}_8$ ) and E) 6 9c-2e  $\sigma$  bonds ( $\text{CuGe}_8$ ); F) 42 2c-2e  $\sigma$  bonds; G) 6 6c-2e  $\pi$  bonds.

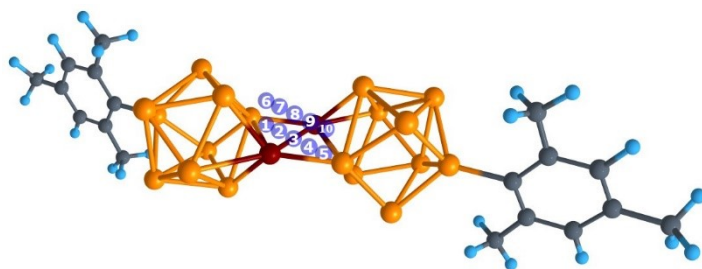


**Figure S12.** The planar  $\text{Cu}_2\text{Ge}_2$  fragment of  $\{[\text{CuGe}_9\text{Mes}]_2\}^{4-}$  with points that were chosen for NICS indices calculations.

**Table S4.** NICS<sub>iso</sub> and NICS<sub>zz</sub> indices calculated at chosen points for {[CuGe<sub>9</sub>Mes]<sub>2</sub>}<sup>4-</sup>.

Point	NICS <sub>iso</sub>	NICS <sub>zz</sub>
1	-44.59	2.11
2	-24.83	14.52
3	-19.45	18.09
4	-24.83	14.52
5	-44.59	2.11
6	-23.99	-15.84
7	-14.11	4.70
8	-10.64	9.05
9	-14.11	4.70
10	-23.99	-15.84

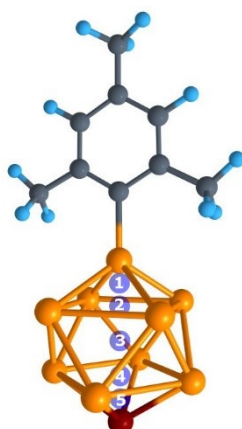


**Figure S13.** The [CuGe<sub>9</sub>Mes]<sub>2</sub><sup>2-</sup> cluster with points that were chosen for NICS indices calculations.

**Table S5.** NICS<sub>iso</sub> and NICS<sub>zz</sub> indices calculated at chosen points for {[CuGe<sub>9</sub>Mes]<sub>2</sub>}<sup>4-</sup>.

Point	NICS <sub>iso</sub>	NICS <sub>zz</sub>
1	-75.31	-32.52
2	-69.15	-62.76
3	-64.43	-63.54
4	-69.27	-64.70
5	-117.55	-103.29

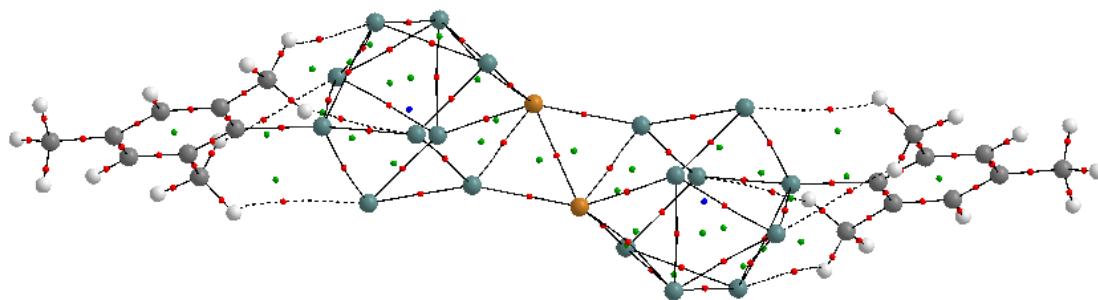


**Figure S14.** Topological analysis of the electron density. Solid lines represent bond paths between bonded atoms and dashed lines bond paths corresponding to weak interactions. Red, green and blue dots are bond, ring and cage critical points, respectively.

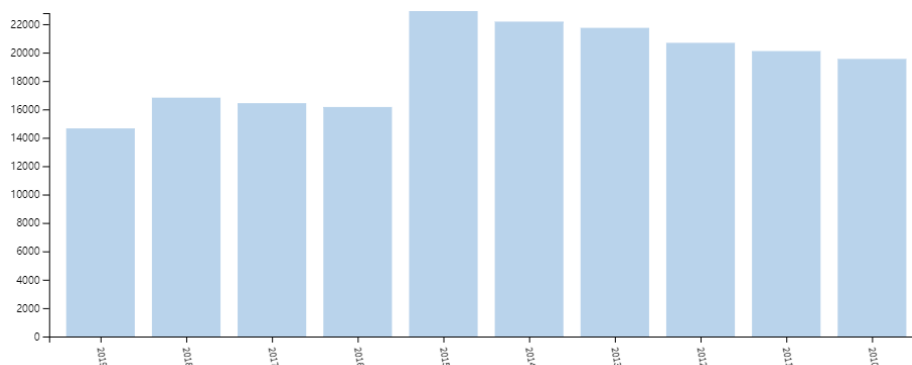


**Figure S15.** Bar graph of search result in Web of Science. It showed 189,844 records for TOPIC: aromatic OR Antiaromatic OR Antiaromaticity OR aromaticity, in the research domain of *Science Technology*.

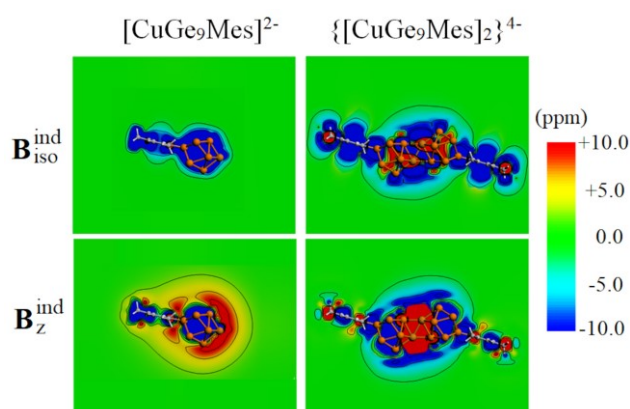


**Figure S16.** Contour plot representation ( $\pm 10$  ppm) of the induced magnetic field accounting for both isotropic and z-orientated field terms. Blue: shielding; red, deshielding.

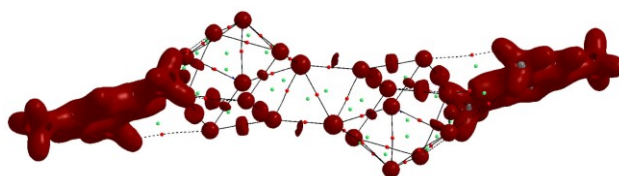


**Figure S17.** Contour plot representation ( $-0.0001$  a.u.) of the Laplacian of the electron density superposing the topological analysis of the electron density. Green dots represent ring critical points.

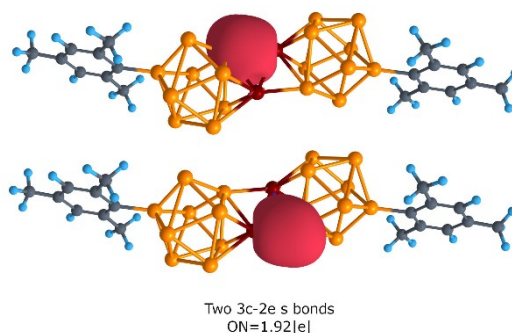


**Figure S18.** Chemical bonding picture of  $\text{Cu}_2\text{Ge}_2$  fragment obtained for  $\{[\text{CuGe}_9\text{Mes}]_2\}^{4-}$  cluster.

## Computational Methods

All structures were optimized at the PBE0/def2-TZVP level of theory. The frequency calculations were performed using the harmonic approximation. The chemical bonding analysis was performed using the AdNDP algorithm as implemented in AdNDP 2.0 and Multifwn 3.7<sup>[5]</sup> codes. The wavefunction was sampled using the def2-TZVP basis set for monomeric

species and def2-TZVP(Cu and Ge atoms)<sup>[6]</sup>/6-311\*G(C and H atoms)<sup>[7]</sup> basis set for the dimeric species. To assess the aromaticity and antiaromaticity with a quantitative parameter, NICS calculations were performed at PBE0/def2-TZVP level. All calculations utilized the Gaussian-09 and Gaussian-16 programs. Induced magnetic field isosurfaces and contour plots were obtained at the related PBE0/TZ2P level of theory by using the ADF suite.<sup>[8]</sup> The topological analysis of the electron density and the electronic aromaticity calculations were performed with AIMall and ESI-3D programs.<sup>[9-12]</sup>

**Explanation of the binding interactions between two monomers in terms of Wade-Mingos electron counting rules.**

The monomer [CuGe<sub>9</sub>Mes]<sup>2-</sup> represents a ten vertex *closo* cluster, which comprises 20 skeletal electrons [(9 Ge) + (2 charges) – (9 Ge lone pairs)] = 36+2-18 = 20 |e|. Thus, the structure lacks two electrons according to the Wade-Mingos rules for *closo* clusters (2n+2, n=10). However, those two electrons are provided by Ge<sub>2</sub>Cu<sub>2</sub> interaction. Therefore, the overall number of skeletal electrons per monomeric subunit in {[CuGe<sub>9</sub>Mes]<sub>2</sub>}<sup>4-</sup> dimer is 22 |e|, which is in agreement with 2n+2 (n=10) electron counting rule.

## References

- [1] E. M. Mayer, S. Gambarotta, C. Florisni, A. Chiesi-Villa, C. Guastin, *Organometallics* **1998**, 8, 1067.
- [2] G. M. Sheldrick, *Acta Crystallogr. Sect. A: Found. Adv.* **2015**, 71, 3.
- [3] O. V. Dolomanov, L. J. Bourhis, R. J. Gildea, J. A. K. Howard, H. Puschmann, *J. Appl. Crystallogr.* **2009**, 42, 339.
- [4] A. L. Spek, *Acta Crystallogr., Sect. D: Biol. Crystallogr.* **2009**, 65, 148.
- [5] T. Lu and F. Chen, *J. Comput. Chem.*, **2012**, 33, 580.
- [6] a) C. Adamo and V. Barone, *J. Chem. Phys.*, **1999**, 110, 6158; b) F. Weigend, R. Ahlrichs, *Phys. Chem. Chem. Phys.*, **2005**, 7, 3297.
- [7] R. Krishnan, J. S. Binkley, R. Seeger and J. A. Pople, *J. Chem. Phys.*, **1980**, 72, 650.
- [8] Amsterdam Density Functional (ADF 2016) Code, Vrije Universiteit: Amsterdam, The Netherlands. Available at: <http://www.scm.com> (Last accessed: Nov. 29th, 2019).
- [9] T.A. Keith AIMall (v. 14.11.23), 2014. TK Gristmill Software, Overland Park KS, USA ([aim.tkgristmill.com](http://aim.tkgristmill.com)).
- [10] E. Matito ESI-3D. IQCC and DIPIC, Donostia (Spain).
- [11] E. Matito, M. Duran and M. Solà, *J. Chem. Phys.*, **2005**, 122, 014109.
- [12] E. Matito, M. Solà, P. Salvador and M. Duran, *Faraday Discuss.*, **2007**, 135, 325.